6th IAHR International Meeting of the Workgroup on Cavitation and Dynamic Problems in Hydraulic Machinery and Systems, September 9-11, 2015, Ljubljana, Slovenia

STEADY AND TRANSIENT PRESSURE MEASUREMENTS ON THE RUNNER BLADES OF A KAPLAN TURBINE MODEL

Arash Soltani Dehkharqani[*†], **Kaveh Amiri**[†], **Michel J. Cervantes**[†‡]

[†]Department of Engineering Science and Mathematics, Lulea University of Technology, Luleå, Sweden

[‡] Department of Energy and Process Engineering, Water Power Laboratory, Norwegian University of Science and Technology, Trondheim, Norway

Abstract

The development of renewable energy sources has increased the need for power regulation. Power system regulation is mainly performed by hydropower plants through load variations. Additional forces are exerted on the runner blades during these load variations. This paper deals with pressure measurement performed on the blades of a Kaplan turbine model under steady state and load variation conditions. Flow behavior and frequency content of the pressure are investigated and compared to find critical condition in terms of pressure fluctuation. The results show that at various operating points and conditions, different regions of the blade are important. During load rejection, a considerable amount of pressure fluctuations are exerted on the runner blades. These results will be used to define experiments to be performed on the corresponding prototype. On the prototype, the loads acting on the runner blades will be investigated at various operation points similar to the model. In addition, the relation between the frequency content on the blades and loads on the main shaft will be investigated. Comparing results from model and prototype eventually would be valuable to explore the flow characteristics in prototype since CFD simulation of prototype is challenging.

Keywords

Kaplan turbine model, load acceptance, load rejection, pressure fluctuation, frequency spectra

1 Introduction

Pressure fluctuations exerted on the runner blades at various operating conditions are essential to determine turbine life expectancy [1]. Different forces and pressure fluctuations may be exerted on the turbine blades and main shaft during load variations compared to steady operation [1]. In recent years Kaplan, Francis and propeller turbines have received much attention from the research community under load variation and steady state [2]. Different operating points, load variations, start-up and shutdown have been studied on a Francis turbine model at the Water power laboratory, NTNU, Norway [3-7]. It has been observed that the pressure fluctuation amplitude during transient operating conditions is higher than during steady state operations. Pressure measurements were performed on the blades of a propeller turbine during steady state and transient operation and frequency analysis was done to find various phenomena's impacting the turbine [1], [8]. Although numerous investigations have been done on hydraulic turbine models, the behavior and nature of the flow in prototype has received less attention in the scientific community.

A measurement campaign on a prototype Kaplan turbine is planned. Its scaled model has been studied experimentally and numerically [9-12]. The procedure of pressure sensor mounting on the prototype runner with possibility of replacing damaged sensors has been proposed [13]. The results of the planned measurement can be used to study scale up effects in water turbine

[*] *Corresponding author*: Department of Engineering Science and Mathematics, Lulea University of Technology, Lulea, Sweden, phone: +46 (0)920 493404, email: arasol@ltu.se

systems. Moreover, the results will be used for CFD simulation of the prototype. Furthermore these experiments may help determine the relation between loads on the blades and torque on the main shaft. Consequently, measuring the strain on the main shaft may help determine the loads on the runner.

In this paper, pressure fluctuations on Kaplan runner blades at three steady operating points (part load (PL), best efficiency point (BEP) and high load (HL)) and six transient measurements between three predefined operating points are analyzed. Regions subjected to high pressure fluctuation during the mentioned conditions are examined.

2 Experimental setup

The full-scale Kaplan turbine Porjus U9 is situated on the Luleå River in the northern part of Sweden. The present study was performed on the 1:3.1 scaled model of the turbine. Fig. 1 presents a sketch of the model which is operated in a closed-loop unit at the hydraulic machinery laboratory of Vattenfall Research and Development, Älvkarleby, Sweden. The runner is composed of 6 blades with a diameter of 0.5 m. The penstock presented in Fig. 1a delivers water to the water supply system which is composed of a spiral casing, 18 unequally distributed stay vanes and 20 equally spaced guide vanes. The turbine operated at a constant rotational speed of 696.3 rpm and a net head of 7.5 m during the measurements.

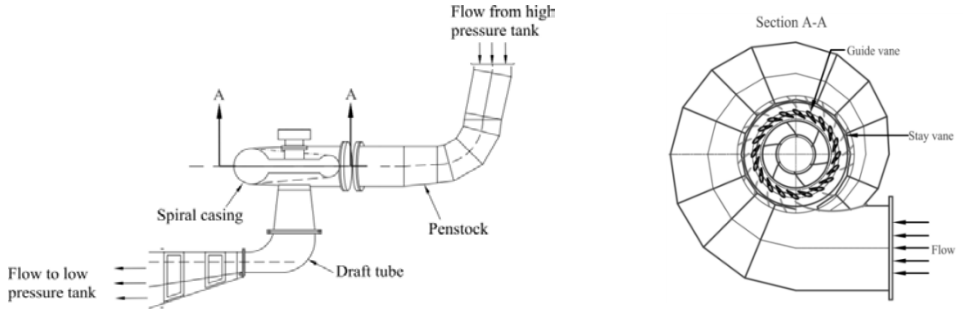

Fig. 1a: Side view of the model; b: top view of the water supply system; spiral casing, stay vane and guide vane (Section A-A). [9]

In this study, the runner characteristics at three different operating points have been investigated. The measurements have been performed at a constant blade angle for each operating point; i.e., during off-cam mode. Operational parameters for the operating points are presented in Tab. 1.

Operating point	**PL**	**BEP**	**HL**
Guide vane angle α_{gv} [°]	20	26.5	32
Volume flow rate (Q) [m^3s^{-1}]	0.62	0.71	0.76
Discharge factor (Q_{ED}) [-]	0.289	0.331	0.354
Speed factor (n_{ED}) [-]	0.676	0.676	0.676
Relative efficiency to BEP ($\eta - \eta_{BEP}$) [%]	-5.6	0.0	-1.6

Tab. 1 Operational condition parameters for the U9 model

The discharge and speed factors are dimensionless numbers defined by the following equations.

$$Q_{ED} = \frac{Q}{D^2\sqrt{gH}} \qquad (1)$$

$$n_{ED} = \frac{nD}{\sqrt{gH}} \qquad (2)$$

The sensors were mounted on two blades, a blade-to-blade channel, on the pressure side of one blade and the suction side of another blade. Six piezoresistive pressure sensors manufactured by Kulite (LL-080 series) were flush-mounted on the pressure side of blade number 1 and six sensors were installed on the suction side of blade number 2. Sensors on the pressure side of blade 1 are shown in Fig. 2. Additional information about the location of the sensors can be found in [9]. The pressure range and natural frequency of the sensors are 0-7 bar and 380 kHz, respectively. Due to the high natural frequency of the sensors compared to the frequencies of interest from the measurements, the investigated frequencies were not affected.

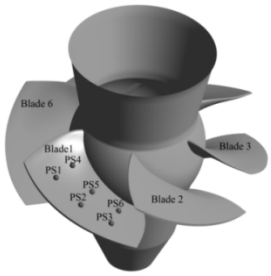

Fig. 2 Schematic of the runner [9].

Two identical telemetry systems, one for each blade, from Summation Research Inc. (SRI-500e) were used for the calibration and measurements. The system was able to transfer data with a frequency up to 17 kHz. The transmitters installed on the rotating shaft, sent signals to the stationary receiver. The analogue signals received by the receiver and pressure sensors on the draft tube cone were directly fed to a data acquisition (DAQ) system with 24-bit resolution; a PXI chassis with four Ni-4472 DAQ cards [9].

The uncertainties of the test rig parameters and sensors are presented in Tab. 2. For additional information see [9].

Instrument	Uncertainty	Position
Hydraulic efficiency	$\leq \pm 0.13\%$	Test rig
Volume flow rate (Q)	$\leq \pm 0.18\%$	Test rig
Head (H)	$\leq \pm 0.04\%$	Test rig
Guide vane angle setting **(α_{gv})**	$\leq \pm 1.3\%$	Test rig
Encoder	0.03º	Test rig
Pressure sensors	$\leq \pm 0.18\%$	Runner blades

Tab. 2 Calibration uncertainties of the test rig parameters and sensors.

3 Data processing

Pressure measurements on the runner blades of the Kaplan turbine model were performed at steady state and load variation operating conditions. At steady state, the model was operated and investigated at PL, BEP and HL. Six load variations between three identical operating points were selected for the unsteady measurements.

The pressure fluctuations are defined as follow:

$$\hat{P}_i(t) = P_i(t) - \overline{P} \qquad (3)$$

Where $P_i(t)$ is the acquired pressure signal, $\overline{P}$ is the time-averaged pressure, t is time, i is the sample index and $\hat{P}_i(t)$ is the fluctuating part of the acquired pressure signal. The data analysis was performed with an in-house developed code, using Welch's method to obtain the frequency content at the various operating conditions. The sampling frequency during all experiments was 4 kHz and the data was recorded for 300 seconds.

4 Results

4.1 Steady measurements

Best efficiency point

Fig. 3 presents the pressure amplitude of the pressure sensors at the BEP for runner and guide vane passing frequencies. The blade tip is affected by the guide vane passing frequency more than other region at the BEP.

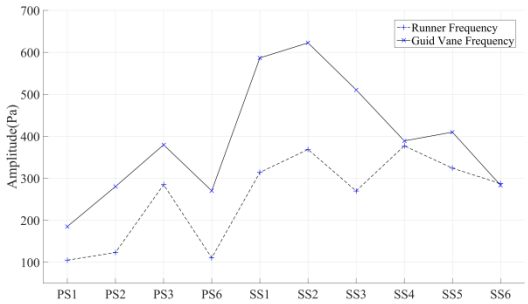

Fig. 3 Pressure amplitude of the pressure sensors at the BEP for runner and guide vane passing frequencies

Runner and guide vane passing frequencies were the dominant frequencies in most of the measurements. Furthermore, $21 \times f^*$ (f^* as the dimensionless runner frequency) was also one of the dominant frequencies, visible in the frequency spectrum of the measured data. For all the steady state cases, the amplitude of the mentioned frequencies increases from the leading edge to the trailing edge on the pressure side. On the other hand, the amplitude of runner frequency decreases chord-wise on the suction side. At the measured operating points, impact of guide vane passing frequency on the suction side at the mid points (SS2, SS5) is maximum compared with adjacent sensors. SS2 has the maximum amplitude for the mentioned frequency.

Part load

Fig. 4 presents the amplitude spectra registered by pressure sensor SS2 at the PL operating point. At PL, $21 \times f^*$ has a significant role in the frequency content. This large frequency amplitude can be seen on the suction side blade tip. Correspondingly, SS2 has the maximum amplitude at this frequency (see Fig. 4 (b)). In addition, the changing pattern of amplitude of the guide vane passing frequency is similar to the BEP. More information about this frequency was explained by Amiri et al. [9].

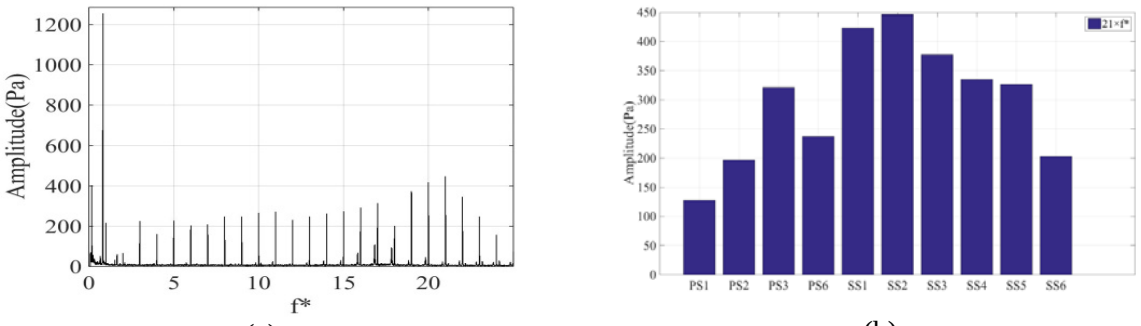

Fig. 4 a) Amplitude spectra of the pressure sensor SS2 b) pressure amplitude with respect to the $21 \times f^*$ *frequency, at the PL operating point*

Two frequencies of $0.171 \times f^*$ and $0.829 \times f^*$ appeared in the amplitude spectra at the PL for all the sensors synchronously, for instance Fig. 4 for SS2. These frequencies were found to

be related to the plunging and rotating modes of the rotating vortex rope (RVR), respectively [9]. The amplitude of the plunging mode is as large as runner and guide vane passing frequency amplitudes. The influence of the other dominant frequencies has been overshadowed by the amplitude of the rotating mode. The amplitude of this frequency is approximately 3 and 6 times larger than the runner and guide vane passing frequencies, respectively. Small peaks found in the amplitude spectra near the dominant frequencies for all of cases due to acquisition system. As the source of these frequencies is known, they were not considered in the analysis.

High load

Fig. 5 illustrates that the trend of the frequency spectrum for HL operating point is similar to the BEP; and the average magnitude of the guide vane passing frequency is smaller than that of for BEP. It can be seen in Fig. 5 that sensor SS1 and SS2 have the maximum magnitude among all the sensors at the runner and guide vane passing frequencies, respectively.

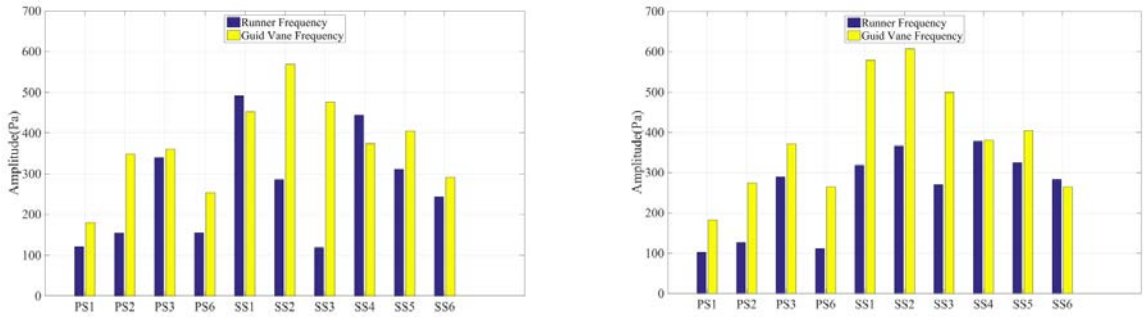

(a) (b)

Fig. 5 Pressure amplitudes with respect to the runner and guide vane frequencies at a) HL, b) BEP

4.2 Transient measurements

Transient measurements have been performed by load acceptance and load rejection tests between three operating points in two different manners; PL_{tr} to BEP, BEP to HL_{tr}, PL_{tr} to HL_{tr}, HL_{tr} to BEP, BEP to PL_{tr} and HL_{tr} to PL_{tr}. Tab. 3 presents the operational parameters of the transient measurements.

Case No.		α_{gv_1}	α_{gv_2}	Q_1	Q_2	H_1	H_2
1	PL_{tr} to BEP	16.2	26.7	0.51	0.69	7.6	7.6
2	BEP to HL_{tr}	26.7	37.5	0.69	0.77	7.5	7.5
3	PL_{tr} to HL_{tr}	16	37.5	0.51	0.77	7.6	7.5
4	HL_{tr} to BEP	37.5	26.6	0.77	0.69	7.5	7.5
5	BEP to PL_{tr}	26.5	16	0.69	0.51	7.6	7.5
6	HL_{tr} to PL_{tr}	37.6	16	0.77	0.51	7.5	7.6

Tab. 3 Operational condition parameters for the unsteady measurements

Guide vane angle during the transient measurement for PL_{tr} and HL_{tr} was not the same as the one during steady operation. The amplitude spectra for some of these cases, which include PL_{tr} and HL_{tr} as an operating point for load acceptance or load rejection, are not quantitatively comparable with that of steady operation. Nevertheless, the magnitude of the dominant frequencies of transient operation can be examined and qualitatively compared with each other.

Case 1

In the transient measurement case 1, the runner and guide vane passing frequencies are the dominant frequencies (See Fig. 6 (a)). Fig. 6 (b) presents the pressure amplitudes at the runner

and guide vane passing frequencies during the load variation. Similar to the steady measurements, on the pressure side of the blade, the amplitude of the runner frequency increases along the chord. The amplitude of the runner frequency measured on the suction side decreases chord-wise. This can be the result of the overlap between the runner blades which decreases pressure pulsation at the trailing edge of the runner. Also, sensors at the position SS2 and SS5 have the maximum magnitude for guide vane passing frequency among the chord-wise arrangement; SS2 has larger amplitude in comparison with SS5 in the all cases.

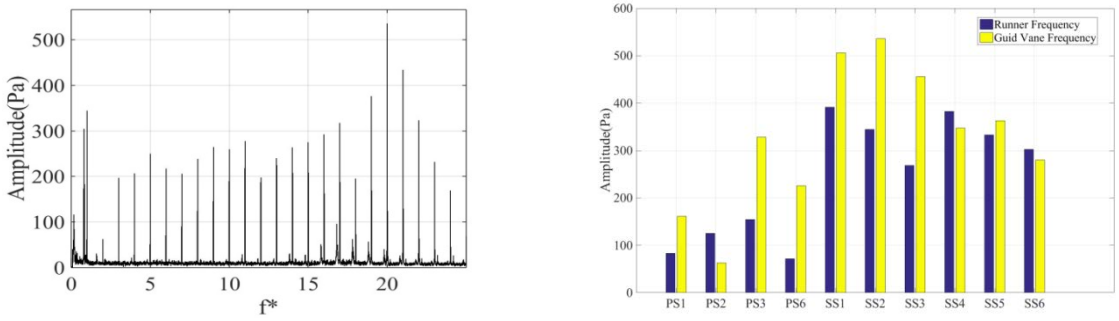

(a) (b)

Fig. 6 a) Amplitude spectra of the pressure sensor SS2, b) pressure amplitudes with respect to the runner and guide vane passing frequencies, during load variation from PL_{tr} to the BEP.

Case 2, 3 and 4

The transient results of the sensors for the runner and guide vane passing frequencies during transient measurement from BEP to HL_{tr} and HL_{tr} to BEP are presented in Fig. 7. Similar results to case 2 have been obtained for case 3. As it can be seen in Fig. 7, the runner and the guide vane passing frequencies dominate the frequency spectrum in the load acceptance and load rejection, respectively. Besides the changing pattern of the amplitude of the guide vane passing frequency during load rejection from HL_{tr} to BEP, it is almost similar to that of the PL_{tr} to BEP. In case 2 and 3, the average amplitude of the runner rotational frequency is higher compare to the other load variations as a result of higher mass flow rate at HL_{tr} compared to the other points.

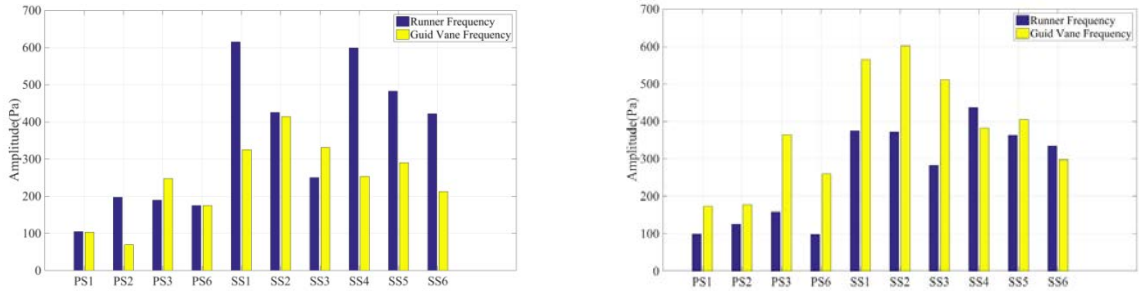

(a) (b)

Fig. 7 Pressure amplitudes with respect to the runner and guide vane passing frequencies; a) BEP to HL_{tr} , b) HL_{tr} to BEP

Case 5 and 6

Two distinct frequencies, which are related to the RVR, were discussed in the results from steady operation at PL. In these two cases, more than 90% of the samples are acquired while the turbine operates at PL_{tr}, unlike other cases. Fig. 8 illustrates pressure amplitude of RVR frequencies (plunging and rotating modes) for case 5. As it can be seen, the dominant frequency in these cases is found to be the rotating frequency of RVR. Furthermore, as presented in Fig. 8, the suction side senses higher amplitude of RVR compared to the pressure

side since flow disturbance comes from the draft tube to the runner [14]. Spectral analysis of these two cases gave quantitatively similar results. It can be realized that since the flow rate in PL_{tr} is less than steady one, the frequencies of plunging and rotating modes of RVR are greater and smaller compared to steady measurements respectively.

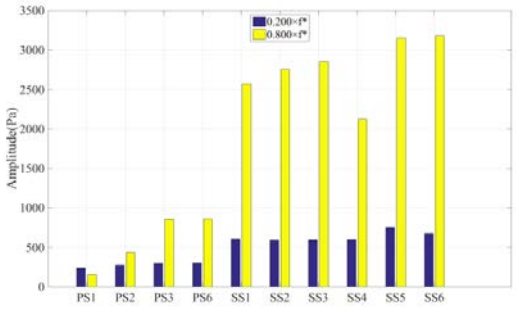

Fig. 8 Pressure amplitudes with respect to the RVR frequencies during load variation from BEP to PL_{tr}

Fig. 9 (a) presents amplitude spectra of the pressure sensors during load variation from HL_{tr} to PL_{tr}. The RVR frequencies have significantly large amplitude than the runner and guide vane passing frequencies in these cases. Fig. 9 (b) illustrates the pressure amplitude of the runner and guide vane passing frequencies for case 6. For the PL steady measurement, the amplitude of the RVR frequency was up to 3 times the average value of the runner frequency amplitude; in the present two cases, this ratio is close to 7. Also, there are large differences between the magnitudes of the runner frequency of the sensor SS5 and others during transient measurement of case 5 and 6. The region close to the runner hub and trailing edge (SS5 and SS6) has the maximum amplitudes among the sensors that are up to 9 and 3 times the average of other sensors, respectively.

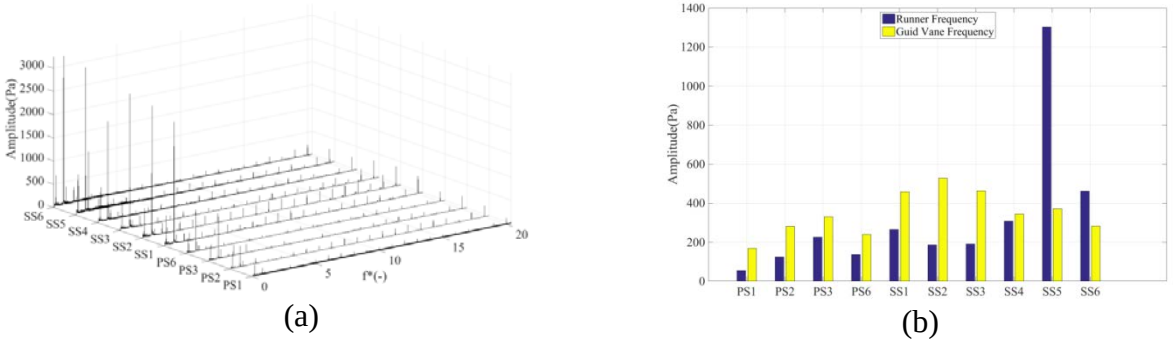

Fig. 9 a) Amplitude spectra of the pressure sensors and b) pressure amplitudes with respect to the runner and guide vane passing frequencies, during load variation from HL_{tr} to PL_{tr}

5 Conclusion

Pressure measurements on two runner blades of a Kaplan turbine model were performed during steady and transient operations. Different critical points have been detected during the measurements. In the steady part, pressure variation at the location SS2 was significant compared to other regions on the runner blades. More importantly, results from transient measurements shows that pressure fluctuations exerted on the runner blades are stronger than steady operating condition. Particularly, load rejection from HL_{tr} to PL_{tr} and BEP to PL_{tr} impact on the pressure fluctuations magnitude. The mid blade region near the hub (SS5) sensed a large pressure fluctuation due to RVR frequency during transient operations from HL_{tr} to PL_{tr} and BEP to PL_{tr}.

6 Acknowledgements

The research presented was carried out as a part of "Swedish Hydropower Centre - SVC". SVC has been established by the Swedish Energy Agency, Elforsk and Svenska Kraftnät together with Luleå University of Technology, The Royal Institute of Technology, Chalmers University of Technology and Uppsala University (www.svc.nu).

7 REFERENCES

[1] S Houde and R Fraser and G D Ciocan and,C.Desch (2012) Part 1 – Experimental study of the pressure fluctuations on propeller turbine runner blades during steady-state operation. IOP Conference Series: Earth and Environmental Science 15: 022004

[2] Trivedi C, Gandhi B, Michel CJ (2013) Effect of transients on Francis turbine runner life: a review. Journal of Hydraulic Research 51: 121-132

[3] Trivedi C, Cervantes MJ, Gandhi B, Dahlhaug OG (2013) Experimental and numerical studies for a high head Francis turbine at several operating points. Journal of Fluids Engineering 135: 111102

[4] Trivedi C, Cervantes MJ, Gandhi B, Dahlhaug GO (2014) Experimental investigations of transient pressure variations in a high head model Francis turbine during start-up and shutdown. Journal of Hydrodynamics, Ser.B 26: 277-290

[5] Trivedi C, Cervantes MJ, Gandhi BK, Dahlhaug OG (2014) Transient Pressure Measurements on a High Head Model Francis Turbine During Emergency Shutdown, Total Load Rejection, and Runaway. Journal of Fluids Engineering 136: 121107-121107

[6] Trivedi C, Cervantes MJ, Dahlhaug OG, Gandhi B (2015) Experimental Investigation of a High Head Francis Turbine During Spin-No-Load Operation. Journal of Fluids Engineering 137: 061106

[7] Trivedi C, Gandhi BK, Cervantes MJ, Dahlhaug OG (2015) Experimental investigations of a model Francis turbine during shutdown at synchronous speed. Renewable Energy 83: 828-836

[8] S Houde and R Fraser and G Ciocan and,C.Desch (2012) Experimental study of the pressure fluctuations on propeller turbine runner blades: part 2, transient conditions. IOP Conference Series: Earth and Environmental Science 15: 062061

[9] Amiri K, Cervantes MJ, Mulu B (2015) Experimental investigation of the hydraulic loads on the runner of a Kaplan turbine model and the corresponding prototype. Journal of Hydraulic Research

[10] Mulu BG, Jonsson PP, Cervantes MJ (2012) Experimental investigation of a Kaplan draft tube – Part I: Best efficiency point. Appl Energy 93: 695-706

[11] Jonsson PP, Mulu BG, Cervantes MJ (2012) Experimental investigation of a Kaplan draft tube – Part II: Off-design conditions. Appl Energy 94: 71-83

[12] Mulu BG, Cervantes MJ, Devals C, Vu TC, Guibault F (2015) Simulation-based investigation of unsteady flow in near-hub region of a Kaplan Turbine with experimental comparison. Engineering Applications of Computational Fluid Mechanics : 1-18

[13] Jansson I, CERVANTES MJ (2007) A method to flush mount replaceable pressure sensors on a 9.3 MW prototype of a Kaplan runner. Proceedings of the 2nd IAHR International Meeting of the Workgroup on Cavitation and Dynamic Problems in Hydraulic Machinery and Systems, Timisoara, Romania, October 24-26, 2007

[14] Amiri K (2014) An experimental investigation of flow in a Kaplan runner: steady-state and transient. Licentiate thesis